Bioorg. Med. Chem. Lett. 33 (2021) 127751

Contents lists available at ScienceDirect

Bioorganic & Medicinal Chemistry Letters

journal homepage: www.elsevier.com/locate/bmcl

Elongation of the side chain by linear alkyl groups increases the potency of salacinol, a potent α-glucosidase inhibitor from the Ayurvedic traditional medicine "*Salacia*," against human intestinal maltase

Katsuki Takashima [a], Mika Sakano [a], Eri Kinouchi [b], Shinya Nakamura [a], Shinsuke Marumoto [c], Fumihiro Ishikawa [a], Kiyofumi Ninomiya [b], Isao Nakanishi [a], Toshio Morikawa [b,*], Genzoh Tanabe [a,b,*]

[a] *Faculty of Pharmacy, Kindai University, 3-4-1 Kowakae, Higashi-osaka, Osaka 577-8502, Japan*
[b] *Pharmaceutical Research and Technology Institute, Kindai University, 3-4-1 Kowakae, Higashi-osaka, Osaka 577-8502, Japan*
[c] *Joint Research Center, Kindai University, 3-4-1 Kowakae, Higashi-osaka, Osaka 577-8502, Japan*

ARTICLE INFO

Keywords:
Salacinol
Kotalanol
α-Glucosidase inhibitor
Salacia
SAR study

ABSTRACT

Four chain-extended analogs (**12a**–**12d**) and two related de-*O*-sulfonated analogs (**13a** and **13c**) by introducing alkyl groups (**a**: R = C_3H_7, **b** R = C_6H_{13}, **c**: R = C_8H_{17}, **d**: R = $C_{10}H_{21}$) to the side chains of salacinol (**1**), a natural α-glucosidase inhibitor from Ayurvedic traditional medicine "*Salacia*", were synthesized. The α-glucosidase inhibitory activities of all the synthesized analogs were evaluated *in vitro*. Against human intestinal maltase, the inhibitory activities of **12a** and **13a** with seven-carbon side chain were equal to that of **1**. In contrast, analogs (**12b**–**12d**, and **13c**) exhibited higher level of inhibitory activity against the same enzyme than **1** and had equal or higher potency than those of the clinically used anti-diabetics, voglibose, acarbose, and miglitol. Thus, elongation of the side chains of **1** was effective for specifically increasing the inhibitory activity against human intestinal maltase.

The roots and stems of plants belonging to the genus *Salacia*, including *Salacia reticulata*, *S. oblonga*, and *S. chinensis*, have traditionally been used in Ayurvedic medicine for treating diabetes. In the late 1990s, salacinol (**1**) was isolated from *S. reticulata*, an Ayurvedic medicinal plant.[1,2] This compound possesses α-glucosidase inhibitory activity that is as potent as that of voglibose and acarbose, which are widely used clinically.[1,2] Owing to this inhibitory activity, compound **1** is assumed to be one of the constituents responsible for the antidiabetic property of *S. reticulata* extract and is an example of a new class of naturally occurring glucosidase inhibitors. The structure of **1**, established by X-ray crystallographic analysis, is quite unique, wherein the ring sulfonium ion is stabilized by the internal sulfate anion, forming a spirobicyclic-like configuration comprising 1-deoxy-4-thioarabinofranosyl cation and 1-deoxy-L-erythrosyl-3-sulfate anion, as shown in Fig. 1.[1,2] Since the discovery of **1**, the related sulfonium sulfates, kotalanol[3] (**2**), ponkoranol[4] (**3**), and salaprinol[4] (**4**), as well as their de-*O*-sulfonated analogs, neosalacinol[5] (**5**), neokotalanol[6,7] (**6**), neoponkoranol[8] (**7**), and neosalaprinol[8] (**8**), have been isolated from the same *Salacia* genus plants. These sulfonium salts, except for **4** and **8**, exhibited the same degree of α-glucosidase inhibitory activity as salacinol (**1**) (Fig. 1). Owing to the α-glucosidase inhibitory activity of its constituent compounds, extracts of *S. reticulata* were used in clinical trials on patients with type-2 diabetes, and were found to be effective and had minimal side effects.[9–13] Because of their intriguing structures and potent α-glucosidase inhibitory activities, much attention has been focused on these natural inhibitors; intensive structure–activity relationship (SAR) studies[14–32] and complete syntheses[8,17,22,23,30–44] of these inhibitors have been reported. In the initial stages of SAR studies focusing on the hydrogen-bonding interactions between the candidate inhibitors and enzyme active sites, side chain stereoisomers of the natural compounds **1**–**6** were synthesized. Evaluation of their activities provided the following insights into the structural features of the side chains that contributed considerably to the inhibitory activity: (a) the 2′*S*-OH and its cooperative role with the C4′-OH is essential for the activity[14]; (b) the *R* configuration of the C4′-OH is imperative for inhibitors bearing a side chain of more than four carbons[15–22]; and (c) the sulfate

* Corresponding authors at: Faculty of Pharmacy, Kindai University, 3-4-1 Kowakae, Higashi-osaka, Osaka 577-8502, Japan (G. Tanabe).
E-mail addresses: morikawa@kindai.ac.jp (T. Morikawa), g-tanabe@phar.kindai.ac.jp (G. Tanabe).

https://doi.org/10.1016/j.bmcl.2020.127751
Received 27 October 2020; Received in revised form 10 December 2020; Accepted 12 December 2020
Available online 19 December 2020

anion at the C3′ position is not required for the activity.[23] Thus, the structural features of the side chain that are necessary for potent α-glucosidase inhibitory activity have been gradually revealed through these SAR studies. However, inhibitors with potency higher than those of the natural sulfonium salts have not yet been synthesized.

In 2010, intensive X-ray crystallographic studies[24] on salacinol (**1**) complexed with the human *N*-terminal catalytic domain of maltase-glucoamylase (hNtMGAM) and/or *in silico* docking[25] of **1** with hNtMGAM were conducted. In these studies, the 3′-*O*-sulfate anion of **1** was found to be constrained by the surrounding hydrophobic residues of the enzyme, which possibly caused negative binding interactions of **1** with the residues. Based on these findings, we synthesized a series of 3′-*O*-alkylated salacinol analogs (**9** and **10**), wherein the sulfate anion in **1** is substituted with a hydrophobic benzyl or alkyl moiety.[26–28] The activities of these analogs (IC_{50} = 0.13–1.7 μM) were better than that of the original compound **1** (IC_{50} = 5.2 μM). The binding modes of **9** and **10** with hNtMGAM indicated another important structural determinant with respect to the side chain—(d) the van der Waals interactions of alkyl and/or benzyl groups on the oxygen atom at the C3′ position of **1** with the enzyme active site significantly enhance the α-glucosidase inhibitory activity. These results suggest that introduction of an appropriate hydrophobic moiety to the side chain of **1** would increase the chances of success during lead-development. Mohan *et al.*[29] synthesized *S*-alkylated sulfonium salts (**11**) with linear aliphatic side chains (n = 2, 6, 12) and evaluated them as inhibitors of recombinant hMGAM. It is noteworthy that these sulfonium salts (**11**) showed moderate inhibitory activities [*Ki* (μM): **11a**, 32 ± 4; **11b**, 51 ± 4; **11c**, 6 ± 1], compared with that of the reference standard, salacinol (**1**) [*Ki* (μM): 0.19 ± 0.02], despite lacking hydroxyl functionalities, which are important side chain structural determinants (a) and (b). Thus, these results suggest that a hydrophobic region distant from the active pocket of the enzyme contributes to substrate recognition. In this study, to further investigate the van der Waals interactions of salacinol analogs with enzymes *via* hydrophobic moieties, four analogs (**12a**, **12b**, **12c**, and **12d**) bearing linear alkyl groups at the terminal carbon (C4′) of the side chain in **1**, as well as the two related de-*O*-desulfonated analogs (**13a** and **13c**) were designed and synthesized. The inhibitory activities of all the analogs (**12** and **13**) against rat intestinal maltase, sucrase, and isomaltase, as well as against human intestinal maltase were experimentally determined to verify the theoretical predictions made computationally.

A schematic of the retrosynthetic analysis is provided in Scheme 1. The target compounds, **12a**–**12d**, **13a**, and **13c**, were prepared by coupling cyclic sulfates (**14a**–**14d**) with a known thiosugar[14] (**15**). The coupling partners (**14a**–**14d**) for **15** were synthesized from a D-arabinose derivative (**16**) *via* three key reactions (i.e., Wittig reaction of **16**, selective olefin reduction of **22**, and cyclic sulfate formation reaction of

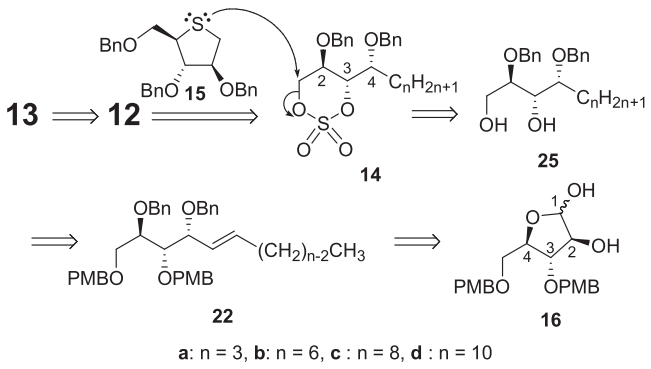

Scheme 1. Retrosynthetic analysis of sulfonium salts **12** and **13.**

25), as the desired stereochemistry at the *C*2, C3, and C4 positions of **14a**–**14d** could be readily produced from **16**.

The key synthon **16** was first prepared in five steps starting from D-arabinose (**17**). The compound **17** was first subjected to selective silylation of the primary hydroxyl with a slight excess of *tert*-butyldiphenylchlorosilane to give a monosilylated product[45] (**18**). Subsequently, **18** was treated with acidic acetone in the presence of anhydrous copper (II) sulfate to get the corresponding acetonide[45] (**19**), desilylation of which with tetra-*n*-butylammonium fluoride led to the formation of a diol[46] (**20**). The total yield of **20** was 56% via the three steps from **17**. Compound **20** was then converted to the key synthon **16** with 42% yield *via* two successive reactions consisting of protection of the two hydroxyls in **20** using *p*-methoxybenzyl chloride (PMBCl) and deacetalization of the resultant PMB ether (**21**). Wittig reactions of **16** with four different alkylidenetriphenylphosphoranes (RCH = PPh_3: R = CH_3, C_4H_9, C_6H_{13}, C_8H_{17}) gave the corresponding alkenes (**22a**–**22d**) as a mixture of geometrical isomers, slightly favoring the *Z* isomer (*Z*/*E* = ~6/1). Without the separation of *Z* and *E* isomers, **22a**–**22d** were subjected to selective hydrogenation of the C=C bond over an ammonia-poisoned palladium catalyst to get the corresponding diols (**23a**–**23d**) with a yield of 96%–98%. After the treatment of **23a**–**23d** with benzyl bromide, the two PMB groups of the resultant dibenzyl ethers **24a**–**24d** were selectively removed using aqueous TFA solution to get the corresponding diols (**25a**–**25d**) via two steps with a yield of 79%–82%. The two hydroxyls of **25a**–**25d** were then treated with $SOCl_2$ in the presence of triethylamine, followed by oxidation of the resultant cyclic sulfites with RuO_4, which was derived by the *in situ* treatment of $NaIO_4$ with $RuCl_3$, to get the target cyclic sulfates **14a**–**14d** in good yields. (Scheme 2).

After synthesizing the cyclic sulfates, **14a**–**14d**, the coupling reaction of **14a** with thiosugar **15** in 1,1,1,3,3,3-hexafluoroisopropanol (HFIP)

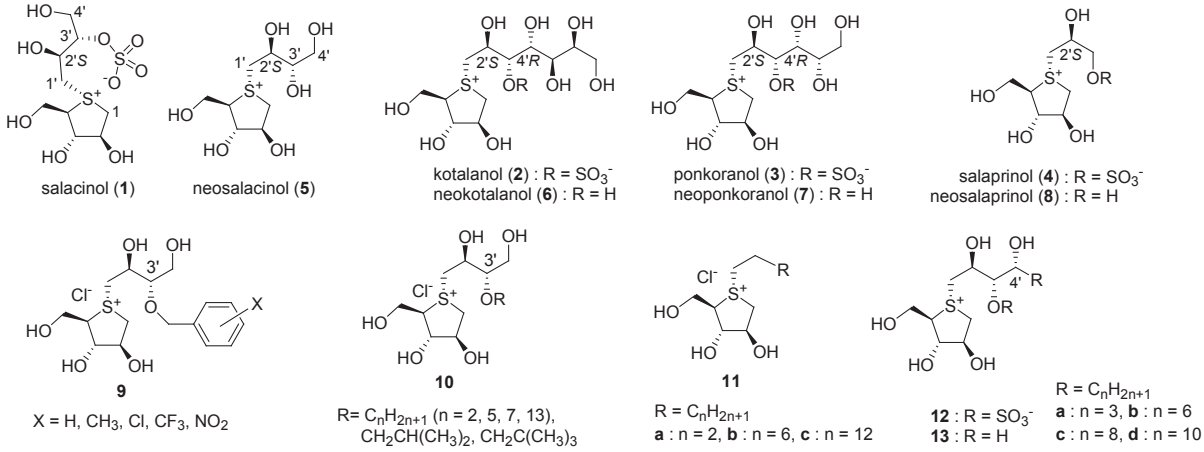

Fig. 1. Structure of the cyclic sulfonium family **1–11** and target sulfonium salts **12** and **13**.

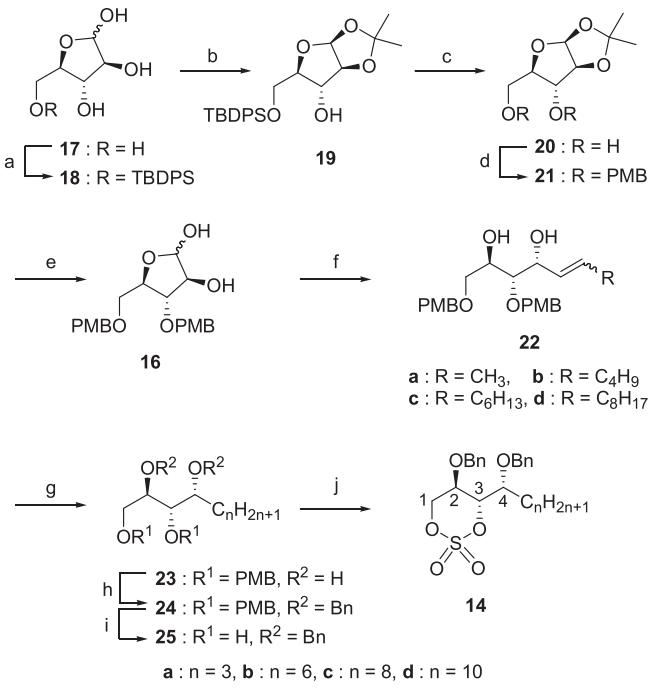

Scheme 2. Reagents and conditions: (a) TBDPSCl, imidazole, DMF, 0 °C–rt; (b) acetone, conc. H_2SO_4, $CuSO_4$, rt; (c) TBAF, THF, 0 °C-rt (56% *via* 3 steps from **17**); (d) PMBCl, NaH, DMF, 0 °C–rt (94%); (e) 10% aq. H_2SO_4, 1,4-dioxane, 50 °C (74%); (f) RCH_2PPh_3Br, *n*-BuLi, THF (R = CH_3, C_4H_9, C_6H_{13}, C_8H_{17}), 0 °C–rt (78–85%); (g) H_2, Pd-C, 28% aq·NH_3, MeOH, rt (96–98%); (h) NaH, BnBr, DMF, 0 °C–rt; (i) 90% aq. TFA, rt, 30 min (79–82% from **23**); (j) $SOCl_2$, NEt_3, CH_2Cl_2, 0 °C, then $NaIO_4$, $RuCl_3$, $NaHCO_3$, CCl_4, CH_3CN, H_2O, 0 °C (78–89% from **25**).

was examined. The reaction proceeded very slowly at 60 °C and was not complete after 1 week of stirring. Raising the temperature led to the decomposition of the starting materials and products, resulting in the formation of a complex mixture. After considerable trial and error, the desired coupled product, **26a**, was obtained with 52% yield by terminating the reaction (after 8 days) before complete consumption of the starting materials. The other coupling reactions with **14b**, **14c**, and **14d** were also conducted in the same manner to get the corresponding coupled products, **26b**, **26c**, and **26d**, with yields of 38%, 42%, and 37%, respectively. The relative stereochemistry between the side chain and the benzyloxymethyl moiety at the C4 position of all the coupled products **26a**–**26d** was determined to be in *trans* (as shown in Scheme 3)

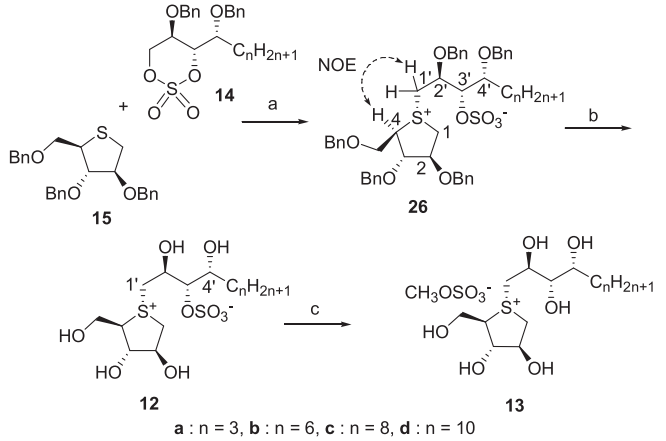

Scheme 3. Reagents and conditions: (a) HFIP, K_2CO_3, 60 °C (33–52%); (b) H_2, Pd-C, 80% aq. AcOH, 60 °C (78–87%); (c) 5% methanolic HCl, 60 °C (82–85%).

on the basis of nuclear Overhauser effect experiments.

Finally, the benzyl protection of **26a**–**26d** was removed by catalytic hydrogenolysis to get the target sulfonium sulfate inner salts **12a**–**12d** with a yield of 78%–88%. Of the four sulfonium sulfate inner salts, **12a** and **12c** were successively treated with methanolic hydrogen chloride to get the corresponding de-*O*-sulfates **13a** and **13c** with a yield of 85% and 82%, respectively. All the synthetic compounds were characterized by the combination of infra-red spectroscopy, ^1H and ^{13}C NMR spectroscopy, and high-resolution mass spectrometry. (See Supplementary data)

In this study, the α-glucosidase inhibitory activities of the newly synthesized sulfonium salts, **12a**, **12b**, **12c**, **12d**, **13a**, and **13c**, were tested using enzymes obtained from rat and human small intestines. The activities were compared with those of the natural inhibitors, **1** and **5**, as well as of the three antidiabetics, voglibose, acarbose, and miglitol, to evaluate the effect of the increasing length of linear alkyl side chain. The experimental values were also compared with the values calculated theoretically using the molecular mechanics/generalized Born volume integration (MM/GBVI) method (Table 1).

First, the inhibitory activities of the compounds against rat α-glucosidases were evaluated. The inhibitory activities of all the sulfonium sulfate inner salts **12a**–**12d** (n = 3, 6, 8, 10) against maltase were satisfactory, with IC_{50} values ranging from 5.4 to 7.7 μM, which are in the same range as those of salacinol (**1**). An extended alkyl side chain seemed to contribute little to the increase in the inhibitory activities against maltase of rat origin. However, the inhibitory activity decreased slightly upon the introduction of an alkyl chain longer than six carbon units, which was evident when the activity of **12a** (n = 3) was compared with that of the related analogs, **12b**–**12d** (n = 6, 8, 10). In contrast, the de-*O*-sulfonated analog (**13c**) having a longer side chain than **13a** (n = 3), showed a superior inhibitory activity (IC_{50} = 2.5 μM) compared with that of **13a** (IC_{50} = 4.8 μM). Thus, it is of interest to note that extension of the chain length from C_3H_7 (n = 3) to C_8H_{17} (n = 8) at the C4′ position of the side chain of neosalacinol (**5**) improves the inhibitory potency.

A side chain length-dependent inhibition of sucrase activity was observed. Of the six synthesized analogs, four (**12b**, **12c**, **12d**, and **13c**) exhibited higher activities than **1** and **5**. Among these, **12c** (n = 8) and **12d** (n = 10) showed potent inhibitory activities (IC_{50} = 0.15–0.17 μM) and were approximately 10-fold more active than **1** and **5** (IC_{50} = 1.3–1.6 μM). Compounds **12a** (n = 3) and **13a** (n = 3) showed inhibitory activities with IC_{50} of 0.73 and 1.4 μM, respectively, which were similar to or slightly higher than those of **1** and **5**. These results indicate that elongation of the alkyl chain more than 8 carbon units (n = 8, 10) at the C4′ position of the side chain in **1** and/or **5** enhances the inhibitory activity against sucrase of rat origin.

In contrast, the inhibitory activities against isomaltase varied depending on the presence of the 3′-*O*-sulfate moiety. Although all the sulfonium sulfate inner salts (**12a**–**12d**) resulted in slightly lower levels of inhibition relative to that caused by **1**, both the de-*O*-sulfonated analogs (**13a** and **13c**) maintained activities almost equivalent to that of **5**, regardless of the chain length. The inhibitory activity of **13c** was approximately 14-fold greater than that of **12c**, although the extent of the increase in inhibitory activity was unpredictable on the basis of the difference in the inhibitory potential of **1** and **12a** from that of **5** and **13a**. Thus, it is noteworthy that the activity enhancing effect of de-*O*-sulfonation was particularly notable for the candidate **13c**, with a longer alkyl chain compared with that of **13a**.

Next, the inhibitory activities against human intestinal maltase were examined and compared with those against rat intestinal maltase. Of the four sulfonium sulfate inner salts (**12a**–**12d**), the three having longer side chains (*i.e.*, **12b**, **12c**, and **12d**; n = 6, 8, and 10, respectively), with ≥ 10 carbon units in total, showed superior inhibitory activities, with IC_{50} values of 1.7, 1.2, and 1.5 μM, respectively; the other analog **12a** (n = 3), having a total of seven carbon units, had a higher IC_{50} of 4.8 μM, as was anticipated based on the *in silico* analysis. These results suggest that introduction of an alkyl chain more than seven carbons long to the side chain of natural sulfonium salt **1** is an effective structural modification

Table 1
E_{bind} (kcal/mol) of sulfonium sulfate inner salts **12a**, **12b**, **12c**, **12d**, de-*O*-sulfonated analogs **13a**, **13c**, natural inhibitors **1** and **5** to hNtMGAM, and their IC_{50} (μM) values against rat and human intestinal disaccharidases.

Entry	Compound	E_{bind}[a]	Rat			Human	Entry	Compound	E_{bind}[a]	Rat			Human
			Maltase	Sucrase	Isomaltase	Maltase				Maltase	Sucrase	Isomaltase	Maltase
1	Salacinol (**1**)	–37.5	5.2[b]	1.6[b]	1.3[b]	4.9[f]	6	**12a** (n = 3)	–39.3	5.4	0.73	2.9	4.8
2	Neosalacinol (**5**)	–34.9	8.0[b]	1.3[b]	0.3[b]	9.0[f]	7	**12b** (n = 6)	–41.1	7.7	0.29	4.8	1.7
3	Voglibose		1.2[c]	0.2[c]	2.1[c]	1.3[f]	8	**12c** (n = 8)	–43.0	7.2	0.15	5.4	1.2
4	Acarbose		1.7[d]	1.5[d]	645[d]	15.2[f]	9	**12d** (n = 10)	–44.4	6.3	0.17	4.4	1.5
5	Miglitol		8.2[e]	0.43[e]	4.6[e]	3.7[f]	10	**13a** (n = 3)	–37.6	4.8	1.4	0.49	5.0
							11	**13c** (n = 8)	–41.9	2.5	0.38	0.40	2.0

[a] Calculation has been performed using the reported scheme[25], [b]lit.[4], [c]lit.[28], [d]lit[53], [e]lit.[26], [f]lit.[54]

for increasing the inhibitory activity by 3–4-fold against human intestinal maltase. These results show that the activities of salacinol-type inhibitors against human intestinal maltase could reach the same level as that of voglibose, which is the most potent among the three antidiabetic medicines showing α-glucosidase inhibitory activity.

The differences between the inhibitory activity of **12a** against human intestinal maltase and those of **12b**–**12d** could be explained based on the results of an *in silico* docking simulation study. The superposition of **12a** (n = 3), **12b** (n = 6), **12c** (n = 8), and **12d** (n = 10) in the hNtMGAM is shown in Fig. 2A, 2B, 2C, and 2D, respectively. The calculations indicated that the binding modes of *C*2′-OH and C4′-OH in analogs **12a**–**12d** with hNtMGAM were similar; by forming three hydrogen bonds, the side chains of all the four compounds satisfied the structural determinants (a)[14] and (b),[15–22] which are essential for the salacinol-type inhibitors to exert potent activity (Fig. 2A–2D, double-headed pink arrows *a*, *b*, and *c*). With respect to the binding mode of another part of the side chain, the C5′–C7′ arm of **12a** shows an intermolecular van der Waals interaction between the terminal methyl group (C7′ position) and the Thr205 residue (Fig. 2A, double-headed orange dotted arrow *d*). The distance between the methyl group and the Thr205 residue was calculated to be approximately 4.07 Å, which was suggested to be enough to induce a van der Waals interaction. However, the inhibitory activity of **12a** [IC_{50} = 4.8 μM] was similar to that of salacinol (**1**) [IC_{50} = 4.9 μM]. No improvement in the inhibitory activity was observed by the introduction of the C_3H_7 group at the C4′ position of the side chain of **1**, although **12a** was predicted to have a superior inhibitory activity compared with that

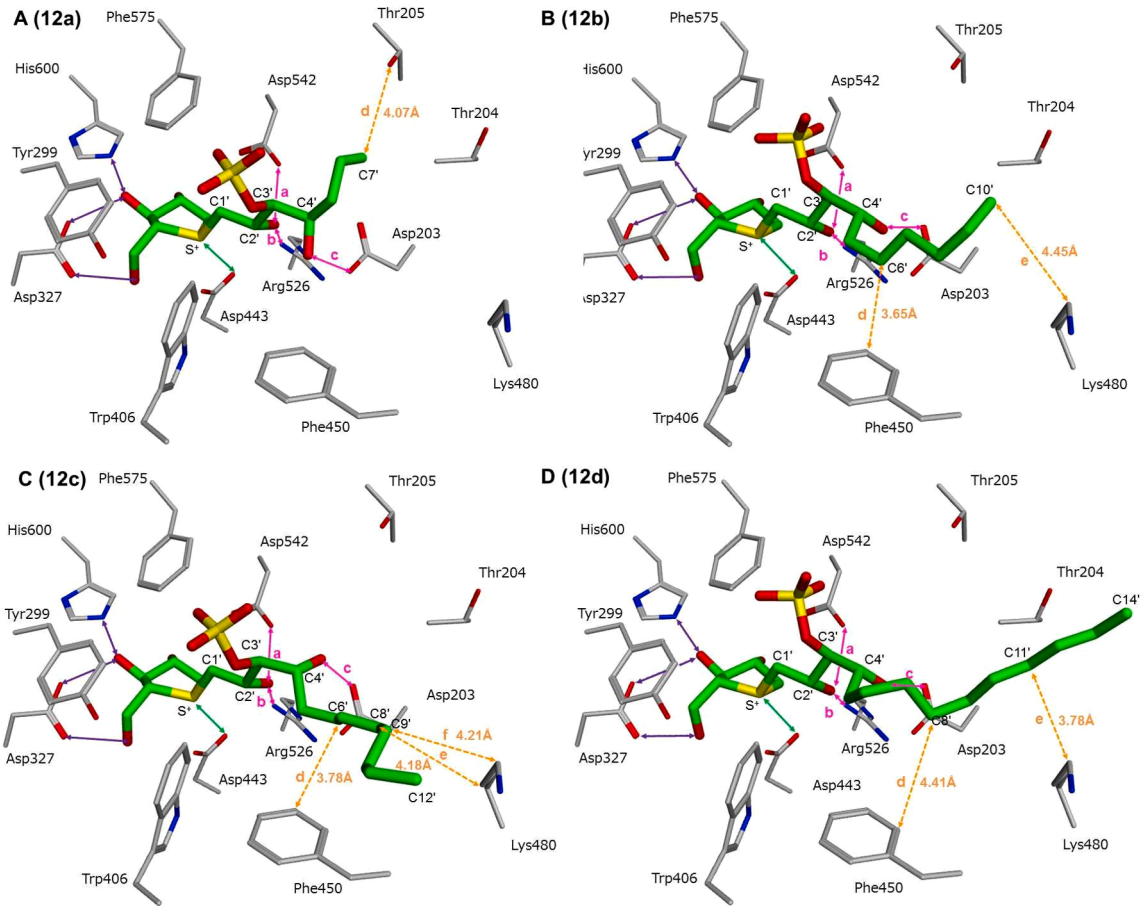

Fig. 2. Superpositions of an analogue **12a A**, **12b B**, **12c C**, and **12d D** in the hNtMGAM active site. Double-headed arrows show hydrogen bonding (purple) and salt bridge (green) of thiosugar moiety with amino acid residues. Double-headed pink arrows a, b, c show distances between *C*2′-OH and C4′-OH in the side chain and amino acid residues (**12a**, *a*: 2.76 Å, *b*: 2.95 Å, *c*: 3.01 Å, **12b**, *a*: 3.21, *b*: 3.49 Å, *c*: 3.52 Å, **12c**, *a*: 2.76 Å, *b*: 3.22 Å, *c*: 3.12 Å, **12d**, *a*: 3.23 Å, *b*: 3.50 Å, *c*: 3.05 Å). Double-headed orange arrows *d*, *e*, *f* show distances between side chain carbons and amino acid residues (**12a**, *d*: 4.07 Å, **12b**, *d*: 3.65 Å, *e*: 4.45 Å, **12c**, *d*: 3.78 Å, *e*: 4.18 Å, *f*: 4.21 Å, **12d**, *d*: 4.41 Å, *e*: 3.78 Å).

of **1** based on *in silico* analysis. Therefore, based on this evidence, we suggest that the stabilization energy associated with the addition of a single van der Waals interaction between the C7′-methyl and Thr205 residue is not sufficient to allow the C5′–C7′ arm to effectively rest on the enzyme-wall near the active site.

The arms of **12b–12d** are arranged differently from that of **12a** to avoid steric repulsion of the longer alkyl chain of the arm from the enzyme wall consisting of Thr205 and Thr204 (Fig. 2B, 2C, 2D). The arms of **12b**, **12c**, and **12d** were observed to contact the amino acid residues, Lys480 and Phe450, which are positioned on the other side of the enzyme wall. Conformational deformations in **12b**, **12c**, and **12d** increase the quality of van der Waals interactions with the enzyme; for example, as depicted for **12b** in Fig. 2B, there are interactions between the methyl carbon at the C10′ position and the hydrophobic portion of Lys480 and between the methylene carbon at the C6′ position and the phenyl ring of Phe450 (double-headed orange arrows *d* and *e* are depicted). The distances *d* and *e* were calculated to be approximately 3.65 and 4.45 Å, respectively, which are sufficient to allow optimal contacts for effective van der Waals interactions with the amino acid residues of the enzyme. Moreover, the side chains of the related analogs (**12c** and **12d**), which also exhibited potent inhibitory activities, were observed to form contacts with the same amino acid residues, Lys480 and Phe450, via a similar binding mode as that of **12c** in the *in silico* docking study. This evidence also supports the notion that long alkyl chains play an important role in binding with the enzyme. Lys480 and Phe450 were found to be important amino acids that contribute to conformational stabilization of the alkyl chain by van der Waals interactions.

Maltase-glucoamylase (MGAM) and sucrase-isomaltase (SI) are responsible for the digestion of terminal starch products remaining after the action of α-amylase. These membrane-bound enzymes are known to contain two catalytic subunits: an *N*-terminal subunit (NtMGAM and NtSI, respectively), which is proximal to the membrane-bound end, and a *C*-terminal luminal subunit (CtMGAM and CtSI, respectively).[47–49] α-Glucosidase catalytic domains in rat are known to be homologous to those in human. For instance, the *N*-terminal catalytic domain of rat maltase-glucoamylase (rNtMGAM) and that of human (hNtMGAM) were reported to share 60% amino acid sequence similarity.[50,51]

The compounds **12b**, **12c**, and **12d** were found to be slightly inferior inhibitors of rat intestinal maltase compared with **12a**, whereas their inhibitory potency against human intestinal maltase was better than that of **12a**. This discrepancy could be attributable to differences in the amino acid sequences of the enzyme between rats and humans, as shown in Table 2.[51,52] The extended side chains of all the potent inhibitors (**12b**, **12c**, and **12d**) were observed to make effective van der Waals interactions with Phe450 and Lys480 in hNtMGAM, as shown in Fig. 2B, 2C, and 2D, respectively. In contrast, one of the favorable interactions of the extended side chains of **12b**, **12c**, and **12d** with rNtMGAM was completely lacking because Lys480 is missing in rNtMGAM. Additionally, Leu444 of rNtMGAM is the amino acid residue corresponding to Phe450 of hNtMGAM. Therefore, it was conceivable that this mutation reduces the van der Waals interaction with **12b**, **12c**, and **12d**, because terminal methyl groups of Leu444 isobutyl residue are less bulky than the phenyl ring of Phe450m and besides, the CH-π interaction was lost. On the other hand, with respect to another catalytic domain CtSI, Arg503 of hNtMGAM was changed to Glu504 in rNtMGAM. Although the residues of Arg503 and Glu504 have opposite electrostatic property, electrostatic appears not to contribute to the stabilization of the side chain of **12b**, **12c**, and **12d** in the enzyme. Thus, the variation of the inhibitory potency of **12b**, **12c**, and **12d** depends on the difference of the amino acid reside of the catalytic domain between hNtMGAM and rNtMGAM.

Table 2
Comparison of amino acid residue of maltase domains between human and rat.[51,52]

	NtMGAM	NtSI	CtMGAM	CtSI
Human	Phe450	Phe450	Phe468	Phe470
Rat	Leu444	Phe450	Phe483	Phe464
Human	Lys480	Lys480	Lys501	Arg503
Rat	–	Lys482	Lys515	Glu504
Human	Thr205	Leu204	Pro200	Pro208
Rat	Thr205	Ile205	Pro216	Pro202

On the contrary, both the de-*O*-sulfonated analogs, **13a** (n = 3) and **13c** (n = 6), showed satisfactory inhibitory activity against human intestinal maltase, with IC_{50} values of 5.0 and 2.0 μM, respectively. It is noteworthy that the inhibitory activity of **13c** was ~5-fold stronger than that of the reference standard **5** (IC_{50} = 9.0 μM), although **13a** was a slightly superior inhibitor than **5**. The elongation of the side chain by long alkyl groups was effective for the de-*O*-sulfonated series. However, based on the results of the *in silico* docking study, it could not be predicted whether **13a** and **13c** would possess the same level of inhibitory activity as the corresponding 3′-*O*-sulfate inner salts (**12a** and **12c**), because, as shown in Fig. 3A and 3B, their alkyl side chains have completely lost the favorable van der Waals interaction with Phe450 that is observed with **12b**, **12c**, and **12c**. Furthermore, the C7′ carbon of **12a** interacts with Thr205 (4.07 Å), but that of **13a** is distant from this residue and has lesser interaction with the nearby Thr204 (4.95 Å). In the case of **12c**, the C8′ and C9′ carbons in the side chain contacted the Lys480 residue with lengths of 4.18 and 4.21 Å, respectively. In contrast, in the side chain of **13c**, only the C8′ carbon had van der Waals interaction with Lys480, although the length (3.83 Å) was slightly shorter than that for the contacts of **12c**. Consequently, the better performance of **13a** and **13c** is suggested to be attributable to the de-*O*-sulfonation effect,[24] which is known to relieve the positional constraint imposed by the bulky hydrophobic residues (*e.g.*, Phe575, Trp406, and Tyr299) surrounding the sulfate moiety at the C3′ position to allow the side chain to make optimal contacts with the enzyme active site.

Better performance of **13a** and **13c** was also observed with respect to the inhibitory activity against rat isomaltase [IC_{50} = 0.40–0.49 μM] compared with those [IC_{50} = 2.9–5.4 μM] of other synthetics (**12a**–**12d**). Of the four catalytic domains, only NtSI exhibits isomaltase inhibitory activity.[47–49] Thus, the difference in the inhibitory activity would be explained by the difference in degree of the relative entropic gain resulting from the hydrophobic interactions between the Ile205 reside of rNtSI (corresponded to Leu204 in hNtSI, see Table 2), and the side chains of inhibitors, since de-*O*-sulfonation caused increases in the hydrophobic surface area of the molecule, making the side chain of **13a** and **13c** more hydrophobic than those of **12a**–**12d**. On the other hand, the difference in the activity against rat sucrase between the C7 alkyl side chain analog (**13a**, IC_{50} = 1.4 μM) and the other four synthetics (**12b**, **12c**, **12d** and **13c**, IC_{50} = 0.15–0.38 μM) with a side chain longer than C7 was noticeable. The *C*- terminus (rCtSI) of the enzyme, which mainly shows sucrase inhibitory activity,[47–49] has a compact residue (Pro202) at a position far from the active cavity. *In silico* calculation indicated that the side chain of **13a** is too short for making van der Waals interactions with Pro202, whereas those of **12b**–**12d** and **13c** are long enough to effectively interact with the residue. Additionally, it was suggested that de-*O*-sulfonation contributed to the attenuation of the van der Waals interactions with another binding site of rCtSI, when the inhibitory activities of **13a** (IC_{50} = 1.4 μM) were compared with that of **12a** (IC_{50} = 0.73 μM). Therefore, given the aforementioned factors, the isomaltase specific inhibition of **13a** may be considerable.

In conclusion, using an *in silico* method, α-glucosidase inhibitors (**12b**, **12c**, **12d**, and **13c**) with higher activities against human intestinal maltase than the seed compound, salacinol (**1**), were effectively designed and synthesized. The activity of **12c**, the most active compound, was approximately 4-fold higher than that of compound **1**. The SAR studies revealed a novel effect of the side chains of the compounds on their inhibitor activities; specifically, the introduction of long alkyl chains to the terminal carbon (C4′) in the side chain of compound **1** and/or **5** was found to contribute to increasing the inhibitory activity. The

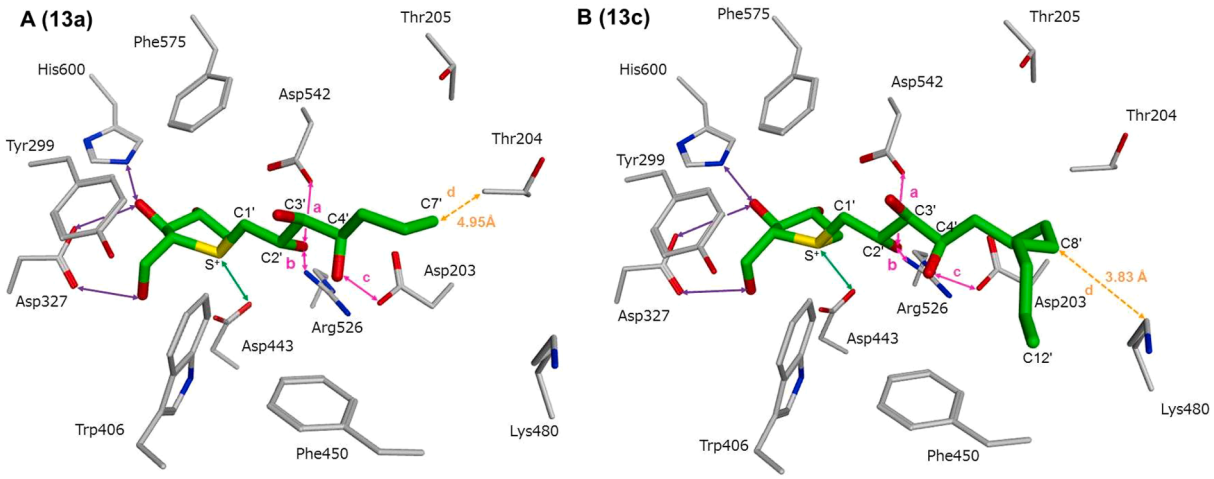

Fig. 3. Superpositions of an analogue **13a A**, **13c B** in the hNtMGAM active site. Double-headed arrows show hydrogen bonding (purple) and salt bridge (green) of thiosugar moiety with amino acid residues. Double-headed purple arrows a, b, c show distances between C2′-OH and C4′-OH in the side chain and amino acid residues (**13a**, *a*: 3.20 Å, *b*: 3.28 Å, *c*: 3.63 Å, **13c**, *a*: 3.29, *b*: 3.32 Å, *c*: 3.93 Å). A double-headed orange arrow *d* shows distance between side chain carbon amino acid residue (**13a**, 4.95 Å, **13c**, 3.83 Å).

van der Waals interactions between carbons (*e.g.*, C6′, C8′, and C9′) in the middle of the long alkyl chain, and amino acid residues, such as Lys480 and Phe450, in the enzyme, contributed to the increase in the inhibitory activity. Moreover, these analogs (**12b**, **12c**, **12d**, and **13c**) were found to be potent inhibitors of rat sucrase. These analogs should be useful for studying the selectivity of sulfonium-type inhibitors against the subunits of α-glucosidases. Further SAR studies to search for analogs of these sulfonium-type inhibitors having stronger α-glucosidase inhibitory activities are currently in progress.

Declaration of competing interest

The authors declare that they have no known competing financial interests or personal relationships that could have appeared to influence the work reported in this paper.

Acknowledgments

This study was supported by a grant from the Hoansha Foundation, Osaka, Japan, 2017–2020 (G.T.) and also supported by a grant-in-Aid for Scientific Research [KAKENHI, Grant Numbers 17 K08377 (G.T.)]. The authors thank financial supports extended by Kobayashi International Scholarship Foundation (T.M.) and the MEXT-Supported Program for the Strategic Research Foundation at Private Universities (T.M.) and by the “Antiaging” Project for Private Universities (G.T and T.M).

Appendix A. Supplementary data

Supplementary data to this article can be found online at https://doi.org/10.1016/j.bmcl.2020.127751.

References

1 Yoshikawa M, Murakami T, Shimada H, et al. *Tetrahedron Lett.* 1997;38:8367–8370.
2 Yoshikawa M, Morikawa T, Matsuda H, et al. *Bioorg Med Chem.* 2002;10:1547–1554.
3 Yoshikawa M, Murakami T, Yashiro K, et al. *Chem Pharm Bull.* 1998;46:1339–1340.
4 Yoshikawa M, Xu F, Nakamura S, et al. *Heterocycles.* 2008;75:1397–1405.
5 Minami Y, Kuriyama C, Ikeda K, et al. *Bioorg Med Chem.* 2008;16:2734–2740.
6 Ozaki S, Oe H, Kitamura S. *J Nat Prod.* 2008;71:981–984.
7 Muraoka O, Xie W, Tanabe G, et al. *Tetrahedron Lett.* 2008;49:7315–7317.
8 Xie W, Tanabe G, Akaki J, et al. *Bioorg Med Chem.* 2011;19:2015–2022.
9 Kobayashi M, Akaki J, Yamashita K, et al. *Jpn Pharmacol Ther.* 2010;38:545–550.
10 Williams JA, Choe YS, Noss MJ, et al. *Am J Clin Nutr.* 2007;86:124–130.
11 Jayawardena MHS, de Alwis NMW, Hettigoda V, et al. *J Ethnopharmacol.* 2005;97:215–218.
12 Kajimoto O, Kawamori S, Shimoda H, et al. *Nippon Eiyo·Shokuryo Gakkaishi.* 2000;53:199–205.
13 Shimoda H, Fujimura T, Makino K, et al. *Shokuhin Eiseigaku Zasshi.* 1999;40:198–205.
14 Muraoka O, Yoshikai K, Takahashi H, et al. *Bioorg Med Chem.* 2006;14:500–509.
15 Tanabe G, Matsuoka K, Yoshinaga M, et al. *Bioorg Med Chem.* 2012;24:6321–6334.
16 Xie W, Tanabe G, Matsuoka K, et al. *Bioorg Med Chem.* 2011;24:2252–2262.
17 Johnston BD, Jensen HH, Pinto BM. *J Org Chem.* 2006;71:1111–1118.
18 Nasi R, Patrick BO, Sim L, et al. *J Org Chem.* 2008;73:6172–6181.
19 Nasi R, Sim L, Rose DR, Pinto BM. *J Org Chem.* 2007;72:180–186.
20 Liu H, Sim L, Rose DR, et al. *J Org Chem.* 2006;71:3007–3013.
21 Liu H, Nasi R, Jayakanthan K, et al. *J Org Chem.* 2007;72:6562–6572.
22 Eskandari R, Kuntz DA, Rose DR, et al. *Org Lett.* 2010;12:1632–1635.
23 Tanabe G, Yoshikai K, Hatanaka T, et al. *Bioorg Med Chem.* 2007;15:3926–3937.
24 Sim L, Jayakanthan K, Mohan S, et al. *Biochemistry.* 2010;49:443–451.
25 Nakamura S, Takahira K, Tanabe G, et al. *Bioorg Med Chem Lett.* 2010;20:4420–4423.
26 Tanabe G, Xie W, Balakishan G, et al. *Bioorg Med Chem.* 2016;24:3705–3715.
27 Tanabe G, Nakamura S, Tsutsui N, et al. *Chem Commun.* 2012;48:8646–8648.
28 Tanabe G, Otani T, Cong W, et al. *Bioorg Med Chem Lett.* 2011;21:3159–3162.
29 Mohan S, Sim L, Rose DR, et al. *Carbohydr Res.* 2007;342:901–912.
30 Mohan S, Pinto BM. *Carbohydr Res.* 2007;342:1551–1580.
31 Xie W, Tanabe G, Xu J, et al. *Mini-Rev Org Chem.* 2013;10:141–159.
32 Mohan S, Eskandari R, Pinto BM. *Acc Chem Res.* 2014;47:211–225.
33 Yuasa H, Takada J, Hashimoto H. *Tetrahedron Lett.* 2000;41:6615–6618.
34 Ghavami A, Johnston BD, Pinto BM. *J Org Chem.* 2001;66:2312–2317.
35 Ghavami A, Sadalapure KS, Johnston BD, et al. *Synlett.* 2003:1259–1262.
36 Jayakanthan K, Mohan S, Pinto BM. *J Am Chem Soc.* 2009;131:5621–5626.
37 Tanabe G, Sakano M, Minematsu T, et al. *Tetrahedron.* 2008;64:10080–10086.
38 Tanabe G, Xie W, Ogawa A, et al. *Bioorg Med Chem Lett.* 2009;19:2195–2918.
39 Tanabe G, Matsuda Y, Oka M, et al. *J Org Chem.* 2016;81:3407–3415.
40 Liu D, Xie W, Liu L, et al. *Tetrahedron Lett.* 2013;54:6333–6336.
41 Ishikawa F, Jinno K, Knouchi E, et al. *J Org Chem.* 2018;83:185–193.
42 Wang Z, Huang Y, Liu D, et al. *Curr Org Chem.* 2018;22:930–935.
43 Huang Y, Gao Y, He W, et al. *Angew Chem Int Ed.* 2019;58:6400–6404.
44 Tanabe G, Ueda S, Kurimoto K. *ACS Omega.* 2019;4:7533–7542.
45 Soares FP, Silva MJ, Doboszewski B. *Carbohydr Res.* 2013;380:143–148.
46 Oliver RM, Rao SP, El-Shenawy HA, et al. *J Org Chem.* 1988;53:3287–3292.
47 Sim L, Willemsma C, Mohan S, et al. *J Biol Chem.* 2010;285:17763–117770.
48 Jones K, Sim L, Mohan S, et al. *Bioorg Med Chem.* 2011;19:3929–3934.
49 Ren L, Cao X, Geng P, et al. *Carbohydr Res.* 2011;346:2688–2692.
50 Maltase-glucoamylase Gene ID: (a) Entrez Gene 312272 [Rattus norvegicus (Norway rat)]; (b) Entrez Gene 8972 [Homo sapiens (human)].
51 Nakamura S, Shimada K, Tanabe G, et al. *Open J Med Chem.* 2017;7:19–28.
52 Nakamura S, Takahira K, Tanabe G, et al. *Open J Med Chem.* 2012;2:50–60.
53 Muraoka O, Morikawa T, Miyake S, et al. *J Nat Med.* 2011;65:142–148.
54 Morikawa T, Akaki J, Ninomiya K, et al. *Nutrients.* 2015;7:1480–1493.